

INTER-AMERICAN TROPICAL TUNA COMMISSION

SCIENTIFIC ADVISORY COMMITTEE

16TH MEETING

La Jolla, California (USA)

02-06 June 2025

DOCUMENT SAC-16 INF-I

**MODELLING THE WELL-LEVEL RELATIONSHIP IN SPECIES PROPORTIONS
BETWEEN EMP PORT-SAMPLING DATA AND OBSERVER DATA FOR THE TUNA
PURSE-SEINE FISHERY IN THE EASTERN PACIFIC OCEAN**

Cleridy E. Lennert-Cody, Cristina De La Cadena, Luis Chompoy, Daniel W. Fuller, Mark N. Maunder and
Alexandre Aires-da-Silva

SUMMARY

As part of the scientific staff's research to improve purse-seine tuna species catch estimation, and in support of the individual-vessel catch threshold program (IVT), the staff are working to develop a model for the well-level relationship between the species composition estimates from the Enhanced Monitoring Program (EMP), and the catch data collected by AIDCP observers. Such a statistical model could be used to predict well-level species catch from observer data for unsampled wells and trips, contributing to methodologies for species catch estimation that can benefit from the 100% observer coverage of IATTC Class-6 vessel trips. Because the current IVT applies only to bigeye tuna (BET), the present study focused on development of a model for the proportion of BET in a well. The data used in this study were paired estimates of the proportion of BET from EMP and observer data, for EMP-sampled wells between March 2023 and December 2024. To explain variability in the relationship between two sets of estimates, mixed-effects models were fitted to the data that included a number of covariates, such as factors that might affect an observer's ability to estimate species composition (e.g., brailer capacity; use of a hooper on the main deck), and random effects for vessel, observer and trip. In general, there was an increasing, positive relationship between the EMP and observer estimates of the proportion of BET in a well. The mixed-effects model with the lowest AIC value included a hopper effect (and interaction), a year effect, and random effects for vessels and trips nested within vessels. The overall effect of a hopper was to rotate the fitted EMP-observer relationship to be closer to the 1-to-1 line (the line that indicates the estimates are exactly equal). This effect is consistent with observers being able to make a better estimate of the proportion of BET in the well when they can more clearly view the catch prior to it being loaded below deck. This overall relationship was found to be significantly modified by vessel-specific effects. In addition, there appeared to be an increased tendency for overestimation by the observer, relative to the EMP, in the second year of the study, which suggests that to use the fitted model to predicted species composition for unsampled wells, port-sampling data would need to be routinely collected. Future work will focus on improving distributional aspects of the model, particularly the assumption of a Gaussian distribution for the random effects. And, models for yellowfin tuna and skipjack tuna will be developed, which is made possible because the EMP data cover all three species of tropical tunas due to the nature of the EMP within-well sampling protocol ([SAC-14 INF-I](#)).

BACKGROUND

In support of the individual-vessel catch threshold program (IVT), set by Resolution C-21-04 (and updated in Resolution C-24-01), the Enhanced Monitoring Program (EMP) was established in 2023 to fulfill the Commission's request to the IATTC scientific staff for the best scientific estimate of bigeye tuna (BET) catch per trip and per vessel. The EMP aims to sample a subset of trips of IATTC Class-6 vessels that had historically high catches of BET in the eastern Pacific Ocean (EPO). Approximately 30 prioritized vessels unloading in Manta and Posorja, Ecuador, are the focus of this effort. Although the EMP samples a specific subset of the Class-6 purse-seine fleet, the data collected by the EMP provide opportunities for research on ways to expand the scientific utility of observer data on tuna catches. This is because these two data sources can be paired at the well level for all EMP-sampled wells, given the 100% observer coverage of Class-6 vessel trips. Sampling by the EMP will continue through December 2025, although the coverage in 2025 is reduced relative to that of 2023-2024 ([SAC-16 INF-H](#)).

This document presents results of an analysis of the well-level relationship between the EMP and observer estimates of the proportion of BET in EMP-sampled wells. The purpose of the analysis was to develop a statistical model of the well-level relationship that could be used to predict well-level species catch from observer data. Developing a model for this relationship has several potential benefits. First, with current funding, it is not possible for the EMP to sample all trips of vessels that might be of interest to the IVT. For unsampled trips of priority vessels, the model could be used to predict the BET catch per trip from observer data. Second, a model between port-sampling data, such as that which would be collected under the protocol of the proposed Integrated Port-Sampling Program (IPSP) ([SAC-16-05](#); [SAC-16 INF-J](#)), and observer data, could allow observer data to be used as part of the fleet-level estimation methods for species catch of all three tropical tuna species. This would be beneficial because collection of port-sampling is not possible in all ports where purse-seine vessels unload EPO catch. Moreover, not all wells and/or trips can be sampled in ports where sampling occurs.

DATA

Two data types were used in this study: port-sampling data and observer data. The port-sampling data were collected by the EMP ([SAC-15 INF-H](#); [SAC-16 INF-H](#)) from March 2023 through December 2024. The EMP sampling focused on trips of IATTC Class-6 vessels that primarily set on tunas associated with floating objects (OBJ sets) in the western region of the EPO. However, wells with OBJ-set catch from elsewhere in the EPO were occasionally sampled. Typically, 6 or 8 wells per trip were sampled. Sampled wells had catch from a single set type (OBJ) and almost exclusively from a single area (3 areas¹: west of 110°W; 95°W-110°W; east of 95°W). For each well, the entire well unloading was sampled with a systematic sampling protocol that selected 1 out of every 30 containers of fish unloaded from the well (details are provided in [SAC-14 INF-I](#); [SAC-14-10](#)). For each container of fish, all fish were identified to species (BET; yellowfin tuna (YFT); skipjack tuna (SKJ); Other). All tropical tuna were individually weighed to the nearest 0.02 kg, or for the largest fish², measured to the nearest mm and the lengths later converted to weight (kg) using species-specific length-weight relationships.

For each well sampled by the EMP, Observer Set Summary³ (Resumen De Lances (RDL), in Spanish) data collected by onboard observers of the AIDCP observer program were obtained to create a paired data set. That is, for each EMP-sampled well, both EMP and RDL estimates of the proportion of BET in the well could be computed. RDL data were used for this study because they contain information on set type, dates and locations of fishing, and catch amounts, by species, for the catch from every set loaded into each well of a trip.

¹ There were 6 wells with catch from east of 95°W and 95°W-110°W, and 11 wells with catch from 95°W-110°W and west of 110°W. For the analysis, the 6 wells were assigned to 95°W-110°W and the 11 wells to west of 110°W.

² Due to the upper weight limitation of the portable scales, which was 30 kg, tunas larger than 28 kg were measured for length ([SAC-15 INF-H](#)).

³ This observer data type is also referred to as observer 'well plan' data.

METHODS

Proportion of BET in the well

For the EMP data, the estimated proportion of BET in the well was computed following the method of [SAC-14-10](#) and Lennert-Cody et al. 2024. Given that there was one systematic sample per well, the estimated proportion of BET in the well was equal to the sum, over sampled containers, of the weight of BET, divided by the sum, over sampled containers, of the weight of tropical tunas. The EMP proportion is an estimate because it is based on a sample of catch from the well.

For the RDL data, the estimated proportion of BET in the well was based on the amount of tunas, by species, from each set that was loaded into the well. The estimated proportion of BET was the sum, over the set amounts in the well, of the weight of BET, divided by the sum, over set amounts in the well, of the weight of tropical tunas. The RDL proportion is considered an estimate because, while the observer monitors all the catch that goes into the well, the observer must still apportion that total well catch, which is assumed known, to species, by eye.

In the modelling that follows, it will be assumed that the EMP and the RDL estimates of the proportion of BET in the well are known without error. This is because it is not possible to obtain an estimate of the variance on either of those proportions from existing data. For the EMP proportions, estimating that variance would require more than one systematic sample per well (to estimate sampling error), which has not been feasible to collect under the current logistical constraints associated with the sampling ([SAC-14 INF-I](#)). For the RDL proportions, it would require information on observer-specific ‘measurement’ error for species identifications and amounts (in weight). However, such calibration data are not available. Simulation studies with high-frequency sample data (one out of every 10 containers were sampled; [SAC-14-10](#)) suggested that when sampling one out of every 30 containers, the sample estimate would be more accurate and precise than the RDL estimate (assuming the one-out-of-10 container data were ‘truth’).

Relationship between EMP and RDL BET proportions

Linear mixed-effect models were used to evaluate the relationship between the EMP and RDL well-level estimates of the proportion of BET. These well-level estimates are ‘paired observations’ (i.e. EMP and RDL estimates for the same well). In this analysis, the EMP proportion of BET was taken to be the response variable and the RDL proportion of BET the independent variable. This was done because the main purpose of the modelling was to develop a model to predict species proportions from RDL data for unsampled wells.

To explain variability in the EMP-RDL well-level relationship, 9 covariates were considered in the analysis, in addition to vessel, observer, and trip (Table 1). There were two categories of covariates, those that were intended to capture aspects that might affect an observer’s ability to estimate catch composition, and those related to operational aspects of the catch that went into the well, in case the paired nature of the data did not adequately control for such factors. Covariates related to the observer’s ability to adequately see the catch were: brailer capacity, the presence/absence of double mesh on the brailer (Figure 1a); presence/absence of a hopper on the main deck (used to sort the catch before it is loaded into the wells (Figure 1b); and, vessel flag (if catch loading practices generally differ among vessel groups). The covariate observer sea days (cumulative days at sea as of time of this study) was intended as a general measure of observer experience. We also included the EMP proportion of small (< 5kg) YFT in the well catch as a proxy for the potential misidentification of YFT as BET by the observer. This covariate was estimated from the EMP data because observers do not estimate the amount of tuna by detailed weight categories (this cannot be used for prediction, but may be informative to understand the process). The operational covariates were the area of the sets associated with the catch (i.e. west of 110°W, 95°W-110°W and east of 95°W), and the trimester and year when the trip was unloaded. The temporal factors were included in

case there was any change over time in the IVT's effect on observers' estimation (e.g. a side effect of the IVT and EMP might be to encourage observers to pay extra attention to species identification). Data on brailer capacity, brailer mesh, and hopper presence/absence were collected by the EMP, as this information is not collected by observers.

The three generic covariates related to data structure (vessel, observer, trip) were included in models in several ways. All were included individually as random effects on the intercept of the relationship between the EMP and RDL estimates). Given the hierarchical structure of the data, i.e. wells within trips and then trips within vessels or observers, nested random effects on the intercept were also considered. In addition, models with random effects on both the intercept and the slope of the EMP-RDL relationship were fitted for all three covariates. Preliminary modelling also fitted models with a random effect for EMP sampler team, but this covariate was dropped from the final analyses because it increased the Akaike Criterion (AIC; Akaike 1974). For sampled trips, including a trip effect in the model would be beneficial for predicting the proportion of BET in the catch of unsampled wells of the same trip. For unsampled trips, the trip effect is useful to control for trip-specific variability, to better estimate the effects of other covariates across trips. It is not, however, directly useful for prediction for wells of unsampled trips. In general, inclusion of a trip effect in the model captures the inherent dependence among wells of the same trip, so that this dependency is correctly handled in, for example, statistical testing. The same applies to inclusion of vessel and observer effects in the model.

The general form of the mixed-effects model, for the i -th observation (well of a trip) within the k -th level of the grouping covariate (i.e. vessel, observer, trip) was

$$g(p_{EMP_{ki}}) = (\beta_0 + b_{0_k}) + (\beta_1 + b_{1_k})g(p_{RDL_{ki}}) + \beta_2 x_{jki} + \dots + \epsilon_{ki}$$

where p is the proportion of BET in the well (EMP, RDL), g refers to a Box-Cox transformation (described in detail below), β s denote fixed effects, x_j are covariates, $\mathbf{b}_k \sim N(\mathbf{0}, \Psi)$ are random effects vectors (independent for each vessel/observer/trip; Ψ structure is general positive definite symmetric, Log-Cholesky parametrization (Pinheiro and Bates 1996)), $\epsilon_{ki} \sim N(0, \sigma^2)$ i.i.d. within-group error, independent of \mathbf{b} . For models with nested random effects on the intercept, the first group of terms in parentheses in the equation above would contain an additional random effect term. The mixed-effects models were fitted with the nlme library (Pinheiro and Bates, 2004, 2024) in R (R Core Team 2024). The estimates of the random effects were the Best Linear Unbiased Predictors (BLUPs). The models were fitted using the default method of restricted maximum likelihood (REML). Models were fitted in a stepwise manner, starting with the random effects models, and then adding other covariates individually to the random effects model with the lowest AIC. Among models that differed by less than 2 units for AIC, the simplest model was selected.

Before fitting the mixed-effects models, the EMP BET proportion estimates were transformed, to better conform to the Gaussian assumption of the models, using a Box-Cox transformation (Box and Cox 1964). The two-parameter Box-Cox transformation, applied to a random variable Y , has the following form (γ not equal to 0):

$$\hat{Y} = \frac{(Y + \delta)^\gamma - 1}{\gamma}$$

where the parameters γ and δ were estimated from the data using the geoR library (Riberio et al. 2024). The parameters were estimated for the EMP proportions and then the same transformation (same estimated parameters) was applied to the RDL proportion to preserve the untransformed relationship between the two estimates. Common transformations for proportions, such as the logit or log-log, were not used because the proportion of BET per well is estimated from weight, not counts of fish.

To evaluate the improvement of vessel random effects for prediction of the well-level proportion of BET, Monte Carlo cross-validation (Simon 2007) was used. The procedure, which is iterative, was repeated 10,000 times. At each iteration, the data were divided into training and test subsets, where the test subset was always 1 well per vessel, for all vessels in the final data set (see below). In other words, for each iteration, the test subset consisted of data from 29 wells, and the training subset was the rest of the data set. The model was fitted on the training subset, and predictions were made on the test subset and back-transformed to the [0, 1] scale. Performance for each iteration was measured by the mean squared error (MSE) (i.e., the sum squared differences between actual EMP proportions and predicted proportions divided by 29); other measures will be considered in future studies. Results were summarized across iterations by the average of the 10,000 MSE values, for predictions at the population level (based on estimated fixed effects only), and separately, for those that included the estimated vessel random effects.

RESULTS

Data summaries

From March 2023 through December 2024, 1,099 OBJ-set wells of 155 trips and 35 vessels sampled by the EMP were considered for this study. Some data was excluded from the analyses as described below. The RDL data for those same wells were collected by 99 observers. Most of the 35 vessels were represented by 1 to 6 trips (Table 2). Of the 99 observers, 88 were represented by only 1 – 2 trips (Table 3). For the mixed-effects modelling, 1,059 wells were available for analysis. There were 40 wells for which data on one or more covariates were not available, and those wells were excluded from the analysis.

Of those 1,059 wells, there were 831 wells for which both the EMP and RDL proportions of BET in the well were greater than zero (Table 4). There were considerably more wells for which the RDL proportion of BET was zero but the EMP proportion was not (143 wells or 13.5% of the 1,059 wells), compared to the number of wells for which EMP proportion was zero but the RDL proportion was not (18 wells or 1.7%) (Table 4). The minimum proportion of BET reported in the RDL data was 0.0087, compared to 0.00034 in the EMP data. Per the EMP data, most of the BET in the sampled wells were small fish (< 5kg). The median proportion BET that was small was 0.90 (inter-quartile range (IQR): 0.69, 1.0).

Some of the covariates considered in this study were better distributed in this particular data set than others (Table 5), which in some cases would be expected given the focus of the EMP. Those covariates well-distributed in the data included presence/absence of double mesh on the brailer, presence/absence of a hopper, and unloading year. About half of the 32 vessels had single mesh brailers and about half the vessels had a hopper. Of the 18 vessels with a hopper, only 4 vessels indicated that the hopper was used for less than 80% of their sets. In addition, the number of wells were fairly equally split among the two unloading years, although sampling in 2023 began in March, so data from the first trimester largely correspond to 2024 unloadings. The relationship between the EMP and RDL proportions of BET, by presence/absence of double mesh on the brailer, presence/absence of a hopper and unloading year, are shown in Figure 2.

Those covariates that were not well-distributed in the data set included brailer capacity, fishing area, and observer sea days. Most brailers were between 7 t – 8 t capacity, with only a few brailers with a capacity of 6 t and 9 t – 10 t (Table 5). As would be expected, most wells were filled with catch from the area west of 110°W. Based on cumulative days at sea, most observers would be considered experienced; the median sea days per observer was 2,099 d (IQR: 1091 d, 3275 d).

The EMP proportion of BET in a well was fairly highly positively correlated with the EMP proportion of the tropical tuna catch that was BET less than 5 kg (Table 6), whereas there was little correlation between the EMP proportion of YFT in the tropical tuna catch that were less than 5kg and the EMP proportion of BET

in the well (Table 6). Most of the YFT catch was small fish (< 5kg), with a median proportion of small YFT of 0.89 (IQR: 0.72, 0.98).

The overall relationship between RDL and EMP proportions of BET per well shows a noisy but positive, increasing relationship (Figure 3). This overall relationship appeared to differ by vessel (Figure 3), with the RDL estimate typically less than the EMP estimate for some vessels (Vessel A), larger than the EMP estimate for other vessels (Vessel C), or spread relatively evenly about the 1-to-1 line for still other vessels (Vessel B). For some vessels, the relationship between the RDL and EMP estimates also varied by trip (Figure 4). In addition, the range of proportions did not necessarily span the interval [0, 1] for all trips. For those trips where very little BET was present in the EMP-sampled wells, per both data sources, the well-level estimates were clustered near the origin. In such cases, the estimated slope for the trip may not be significantly different from zero, and thus the data of the trip only provide weak information on what might have been the slope of the relationship, were more BET to have been present in the catch of those wells.

Mixed-effects modelling

Preliminary modelling efforts attempted to use data from all of the 1,059 wells. However, inclusion of the wells with an RDL proportion of BET equal to zero led to artifacts when modelling the data because of the separation between zero and positive RDL values (along the x-axis, Figure 5) once the data had been transformed (see below). Therefore, for the final analysis, the data were limited to the 849 wells with an RDL proportion of BET greater than zero (Table 4). In addition, data for 12 trips were dropped because each of those trips was represented by only 1 - 2 wells, contributing relatively little information on a trip-specific linear relationship. Thus, for the final analysis, a total of 830 wells (about 78% of the full 1,059-well data set) from 127 trips of 29 vessels were retained, with each trip in this trimmed data set represented by at least 3 wells. The results from the final analysis were not substantially different from preliminary results based on the larger data set of 1,059 wells, although model diagnostics were somewhat improved. For the trimmed data set, the parameter estimates for the Box-Cox transformation were $\gamma = 0.364447$ and $\delta = 9.570761e-06$.

Among the random effects included in the analysis (Table 7), models with a trip-level random effect provided the greatest reduction in AIC. For models with nested random effects, trips effects nested within vessel effects provided a greater reduction in AIC than trips effects nested within observers. This is not surprising considering that most observers were represented by only 1 – 2 trips, which were almost always on different vessels. Given these results, and because vessel-level and trip-level effects on the intercept was the simplest representation of the nested structure of the data, subsequent model fitting with the other covariates only included these nested random effects.

Among the other covariates included in the study, only two provided a substantial decrease in the AIC: presence/absence of a hopper and unloading year (Table 7). The lowest AIC, among the fitted models (a value of 458), was obtained with a model that included a hopper effect on both the intercept and RDL slope, and an unloading year effect on the intercept (in addition to the random effects on the intercept of vessels and trips nested within vessels). The AIC of this model was 9 units below the AIC of the model with only nested random effects for vessel and trip (a value of 467).

At the population level, the overall effect of a hopper was to rotate the estimated relationship between the EMP and RDL proportions of BET to be more similar to the 1-to-1 line (Table 8a, Figure 6). On the scale of the Box-Cox transformation, the added contribution to the slope when a hopper was present was 0.21, increasing the slope from 0.75 to 0.96. For the back-transformed relationships (Figure 6b), when no hopper was present, the tendency was for increased overestimation by the RDL, relative to the EMP, over most of the [0, 1] range (compare dashed and solid curves, within year); at small proportion values (less than about 0.2), the curves without a hopper are slightly above those with a hopper (by year), with the EMP estimates

being slightly larger than the RDL no-hopper estimates for 2023. Taking into account the year effect on the intercept, both curves, with and without a hopper, are rotated such that the relationship for 2024 represents greater overestimation by the RDL, compared to the relationship for 2023 (compare dashed lines, and separately, solid curves).

Estimated vessel random effects (Figure 7) will modify the population-level curves shown in Figure 6. Using 2023 as an example, and the three example vessels (Figures 3 – 4), the estimated overall random effect for Vessel B was positive but relatively small (0.0812), which leads to a vessel-specific curve that is close to the 1-to-1 line (Figure 8). For Vessels C and A, the estimated overall random effects were relatively large and negative (Vessel C; -0.1741) or large and positive (Vessel A; 0.2217), indicating overestimation by the RDL data for Vessel C and largely underestimation by the RDL for Vessel A, relative to the EMP (Figure 8). Across all vessels, based on the Monte Carlo cross-validation applied to the data of both years, there was a 15% decrease in the mean squared error when the predicted proportion of BET in a well included the vessel effect, as compared to the population-level prediction.

DISCUSSION

This study developed a mixed-effects model for the relationship between EMP and RDL estimates of the proportion of BET in a well. Among those covariates considered, the presence of a hopper, the unloading year, and vessel and trip random effects contributed to substantially reducing the AIC. For those vessels that had a hopper onboard, the RDL estimates were more similar to the EMP estimates, consistent with observers being able to make more accurate estimates of catch amounts by species when they have a better view of the catch before it is loaded below deck. This overall relationship was found to be significantly modified by vessel-specific effects. In addition, there appeared to be an increased tendency for overestimation by the RDL, as compared to the EMP, in the second year of the study. This change could be related to an effect of the EMP and the IVT on observers' approach to tuna species catch estimation (e.g. more focus on not underestimating bigeye tuna). If so, the results suggest that to use the EMP-RDL relationship to predict catch composition for unsampled wells, port-sampling data would need to be routinely collected. Moreover, results suggest that routine collection of EMP-RDL data for each vessel could lead to improved prediction because of vessel-specific effects. Although this study focused on BET, similar studies will be conducted for YFT and SKJ, which is made possible because the EMP collected data on all three tuna species in each sampled container of a well (Figure 9).

Because the EMP data represent an opportunistic data set with respect to model development for an EMP - RDL relationship, future modelling could benefit from improved covariate information. For example, the use of a hopper in the model was in terms of presence/absence on the vessel level. This is because the use of a hopper on a set-by-set basis is presently not known (i.e. use at the well level). In addition, observers are generally not placed on the same vessel more than once in two years, and thus, the trip effect in our models likely includes any observer-vessel interaction, with little ability with these data to identify observer-specific effects. The type of port-sampling data that would be collected under the proposed IPSP for fleet-level species catch estimation ([SAC-16-05](#); SAC-16 INF-J), would generate appropriate well-level data with more trips per observer, and a broader range of vessels and purse-seine set types, improving model development for a port-sampling – observer species composition well-level relationship.

Further improvements to the EMP-RDL model will include improving distributional aspects. Model diagnostics (Figure 10) suggest that the model fits the data reasonably well, but improvements could be made with respect to the Gaussian assumption for the random effects. Fitting the model to each year separately (Table 9, Figure 11) led to similar estimated fixed effects, but the vessel-level random effects meet the Gaussian assumption better for 2023, as compared to 2024. Other random effect distributions will be explored. Also, the possibility of fitting the model to data of wells for which both the EMP and RDL

estimates were greater than zero also will be explored, given that the EMP was almost always positive when the RDL was positive (Table 4). This would make it possible to consider other transformations for the data, such as the isometric log-ratio transformation (Egozcue et al. 2003). Vessel random effects that vary by year will also be explored because of differences for some vessels by year. For example, for Vessel A, the only trip sampled in 2024 departs from the pattern for most of its trips in 2023 of underestimation by the RDL (Figure 4). The estimated random effects for this vessel from models fitted separately to each year were 0.2208 for 2023 and 0.0494 for 2024. We note that while the random effects distributions and residuals appear short-tailed, relative to a Gaussian distribution, which would tend to overestimate the significance of fixed effects, the estimates of the fixed effects appear largely unaffected (compare estimated coefficients and p-values for the full model to those from model fits by year; Tables 8 – 9).

Additional improvements to the model, through the incorporation of other covariates will be attempted. The magnitude of the within-group distribution standard deviation is larger than the standard deviations of the vessel and trip random effects (Table 8b), suggesting that improvements to model fit through other covariates, and/or more detailed information on the vessel-level covariates already considered (e.g. hopper use), should be explored. At present, observers do not record set-level data on operational characteristics such as the use of a hopper. More generally, observers do not collect data on the presence of a hopper, double mesh on the brailer or brailer size. At the vessel level, this covariate information was collected by the EMP for this study. Information on these and other operational covariates would be beneficial for future research if they could be collected by observers at the set-level (hopper use) or trip level (brailer capacity, dimensions, and mesh characteristics). (The EMP attempted to collect data on brailer dimensions, but was not able to do so for all of the vessels it sampled.) Finally, vessel company might be a more informative covariate than vessel flag and would be worthwhile to include in future models. Vessel company was not used in the present study because it was not available for all vessels at this time of this analysis.

Developing a model for a port-sampling – observer well-level relationship for tuna species, or possibly port-sampling – logbook well-level relationship, has several benefits for science and management. First, in the presence of an IVT, with observer or logbook data, the model could be used to estimate the species proportions in unsampled wells(trips) for sampled vessels, to produce trip-level species estimates. Estimates for wells for which the observer or logbook species estimates are 0 could be based on the average port-sampling estimates from sampled wells for which the observer (logbook) estimates were zero. It might be possible to develop a model with covariates to estimate the proportion of BET in the well when the RDL estimate was zero. Second, a well-level model could be incorporated into a larger plan to develop a model-based methodology for estimation of fleet-level species catch composition that draws on multiple data sources to improve species catch estimation ([SAC-16-05](#); SAC-16 INF-J).

ACKNOWLEDGEMENTS

The authors extend a special thank you to Jennifer Aguilar, Grace Álvarez, Iván Borbor, Carlos Bravo, Jairon Cabrera, Grecia Cedeño, David Crespo, Pablo Delgado, Jonathan Gaibor, Juan Galarza, José Guillén, Richard Lindao, Javier Mejía, James Méndez, Diego Montehermoso, Andrea Montenegro, Marcos Muñoz, Luis Ortiz, Darío Quimi, Shanelka Quiñonez, Alex Santana, Diego Ureta, Wellington Vásquez, Víctor Vincés, Ledin Vizueta, Robinson Zambrano, Tommy Zamora and Alisson Zúñiga for their dedication to collection of high-quality port-sampling data, Jessenia Gilces for data review and data entry, to the industry and national authorities for their support and collaboration, Ernesto Altamirano for discussions on factors that might affect an observer’s ability to accurately estimate species composition, and Mihoko Minami for discussions on statistical transformations to achieve normality.

REFERENCES

- Akaike, H. 1974. A new look at the statistical model identification. *Autom. Control, IEEE Trans.* 19, 716–723.
- Box, E.P. and Cox, D.R. 1964 An analysis of transformations. *Journal of the Royal Statistical Society, Series B.* 26 (2): 211–252.
- Egozcue, J.J., Pawlowsky-Glahn, V., Mateu-Figueras, G. and Barceló-Vidal, C. 2003. Isometric logratio transformations for compositional data analysis. *Mathematical Geology* 35: 279-300.
- Lennert-Cody, C.E., De La Cadena, C., McCracken, M., Chompoy, L., Vogel, N.W., Maunder, M.N., Wiley, B.A., Altamirano Nieto, E., Aires-da-Silva, A. 2024. Within-well patterns in bigeye tuna catch composition and implications for purse-seine port-sampling and catch estimation in the Eastern Pacific Ocean. *Fisheries Research*. <https://doi.org/10.1016/j.fishres.2024.107079>
- Pinheiro J, Bates D, R Core Team 2024. nlme: Linear and Nonlinear Mixed Effects Models_. R package version 3.1-165, <https://CRAN.R-project.org/package=nlme>
- Pinheiro JC, Bates DM 2004. _Mixed-Effects Models in S and S-PLUS_. Springer, New York. <https://doi.org/10.1007/b98882>
- Pinheiro, J.C. and Bates, D.M. 1996. Unconstrained parametrizations for variance-covariance matrices. *Statistics and Computing* 6: 289-296.
- R Core Team 2024. _R: A Language and Environment for Statistical Computing_. R Foundation for Statistical Computing, Vienna, Austria. <https://www.R-project.org/>
- Ribeiro Jr PJ, Diggle P, Christensen O, Schlather M, Bivand R, Ripley B. 2024. _geoR: Analysis of Geostatistical Data_. R package version 1.9-4. <https://CRAN.R-project.org/package=geoR>
- Simon, R. 2007. Resampling strategies for model assessment and selection. In: *Fundamentals of Data Mining in Geonomics and Proteomics*. Dubitzky, W., Granzow, M., Berrar, D., Eds. Springer. pp. 173-186.

TABLE 1. Covariates used in the mixed-effects modelling.

Variable	Description	Level	Type
Fixed effects			
Brailer capacity	Capacity (metric tons) of the container used to load fish from within the purse-seine net onto the vessel.	Vessel	Numerical
Double mesh	Presence/absence of double mesh on the brailer.	Vessel	Categorical
Hopper	Presence/absence of a hopper used to sort catch on the deck prior to loading into the wells.	Vessel	Categorical
Observer sea days	Cumulative number of days at sea for each observer	Overall	Numerical
Small YFT	Proportion of well catch that was small (< 5 kg) YFT	Well	Numerical
Catch area	Set location corresponding to the well catch (west of 110W; 95W – 110W; east of 95W)	Well	Categorical
Unload trimester	Trimester unloading started: months 1-4; 5-8; 9-12	Trip	Categorical
Unload year	Year catch was unloaded: 2023; 2024	Trip	Categorical
Vessel flag	Country of vessel registry	Vessel	Categorical
Random effects			
Vessel	Intercept/slope		
Observer	Intercept/slope		
Trip	Intercept/slope		

TABLE 2. Number of trips per vessel.

Trips per vessel	1	2	3	4	5	6	7	8	10	12	13	14
Number of vessels	8	1	10	2	5	3	1	1	1	1	1	1

TABLE 3. Number of trips per observer.

Trips per observer	1	2	3	4	5
Number of observers	57	31	9	1	1

TABLE 4. Contingency table of wells, according to whether the estimated proportion of BET in the well was greater than zero (EMP>0; RDL>0) or equal to zero (EMP = 0; RDL = 0), for both unloading years combined and by unloading year.

Number of wells	RDL>0	RDL=0	Total
2023 and 2024			
EMP > 0	831	143	974
EMP = 0	18	67	85
Total	849	210	1059
2023			
EMP > 0	435	39	474
EMP = 0	6	25	31
Total	441	64	505
2024			
EMP > 0	396	104	500
EMP = 0	12	42	54
Total	408	146	554

TABLE 5. Distribution of values in the data set for some covariates. “ECU”: Ecuador; “ESP”: European Union; “PAN”: Panama; “NIC/SLV/USA”: Nicaragua/El Salvador/United States.

Brailer capacity (t)	6	7	8	9	10
Number of vessels	2	9	15	4	2
Double mesh on brailer	No	Yes			
Number of vessels	13	19			
Hopper	No	Yes			
Number of vessels	14	18			
Vessel flag	ECU	ESP	PAN	NIC/SLV/USA	
Number of vessels	16	4	8	4	
Area	East of 95°W	95°W-110°W	West of 110°W		
Number of wells	60	140	859		
Trimester well unloaded	1	2	3		
Number of wells	253	444	362		
Year well unloaded	2023	2024			
Number of wells	505	554			

TABLE 6. Pearson correlations among covariates related to proportion of well catch by species, and in the case of BET and YFT, the proportion of the tropical tuna catch that was small (< 5 kg) fish. 'p_spp': proportion of the species in the well catch.

	EMP p_BET	EMP p_YFT	EMP p_SKJ	EMP proportion of BET+YFT < 5 kg in the total catch	EMP proportion of BET < 5 kg in the total catch	EMP proportion of YFT < 5 kg in the total catch	RDL p_BET	RDL p_YFT	RDL p_SKJ
EMP p_BET	1								
EMP p_YFT	0.12	1							
EMP p_SKJ	-0.8	-0.69	1						
EMP proportion of BET+YFT < 5 kg in the total catch	0.5	0.67	-0.77	1					
EMP proportion of BET < 5 kg in the total catch	0.71	0.36	-0.73	0.8	1				
EMP proportion of YFT < 5 kg in the total catch	0.03	0.7	-0.44	0.74	0.18	1			
RDL p_BET	0.74	0.19	-0.66	0.37	0.47	0.08	1		
RDL p_YFT	0.25	0.75	-0.63	0.57	0.41	0.48	0.15	1	
RDL p_SKJ	-0.68	-0.59	0.85	-0.61	-0.58	-0.34	-0.81	-0.71	1

TABLE 7. Mixed-effect models fitted to the data for which the RDL proportion of BET was greater than zero. p_EMP: EMP proportion of BET in the well; p_RDL: RDL proportion BET in the well. For covariates that are factors, the AIC for the main effect and main effect with interaction are separated by a semicolon. In the model formulae, “*” indicated main effect and interaction; “~1|” indicates the random effect applies to the intercept. Nested random effects are separated by a comma. “***”: indicates model shown in Table 8 and Figures 6 - 8.

Model	AIC
Box-Cox(p_EMP) ~	
1, random = ~1 vesno	1341
1, random = ~1 obscede	1252
1, random = ~1 tripno	1133
1, random = ~1 vesno, ~1 tripno	1135
1, random = ~1 obscede, ~1 tripno	Non-PD Var-Cov
Box-Cox(p_RDL), random = ~1 vesno	604
Box-Cox(p_RDL), random = ~1 obscede	565
Box-Cox(p_RDL), random = ~1 tripno	472
Box-Cox(p_RDL), random = ~1 vesno, ~1 tripno	467
Box-Cox(p_RDL), random = ~1 obscede, ~1 tripno	474
Box-Cox(p_RDL), random = ~ p_RDL vesno	593
Box-Cox(p_RDL), random = ~ p_RDL obscede	563
Box-Cox(p_RDL), random = ~ p_RDL tripno	474
Box-Cox(p_RDL), random = ~ p_RDL vesno, ~1 tripno	465
Box-Cox(p_RDL), random = ~ p_RDL obscede, ~1 tripno	No convergence
Box-Cox(p_RDL) + brailer size, random = ~1 vesno, ~1 tripno	473
Box-Cox(p_RDL)+double mesh, random = ~1 vesno, ~1 tripno	472; 477
Box-Cox(p_RDL) +hopper, random = ~1 vesno, ~1 tripno	471; 462
Box-Cox(p_RDL) + trimester, random = ~1 vesno, ~1 tripno	475; 482
Box-Cox(p_RDL) + year, random = ~1 vesno, ~1 tripno	461; 466
Box-Cox(p_RDL) + vessel flag, random = ~1 vesno, ~1 tripno	485; 492
Box-Cox(p_RDL) + area, random = ~1 vesno, ~1 tripno	480; 490
Box-Cox(p_RDL) + observer cumulative sea days, random = ~1 vesno, ~1 tripno	489
Box-Cox(p_RDL) + proportion small YFT, random = ~1 vesno, ~1 tripno	470
Box-Cox(p_RDL) *hopper + year, random = ~1 vesno, ~1 tripno	458**
Box-Cox(p_RDL) + hopper*year, random = ~1 vesno, ~1 tripno	466
Box-Cox(p_RDL) *year + hopper, random = ~1 vesno, ~1 tripno	470
Box-Cox(p_RDL) *hopper*year, random = ~1 vesno, ~1 tripno	469

TABLE 8. (a) Estimated fixed effects and random effect distribution standard deviations (s.d.) obtained for the mixed-effect model with an AIC of 458 in Table 7. Vessel and trip random effects were on the intercept, with trips nested within vessels. For random effects, approximate 95% CIs and estimates for the s.d. The fitted coefficients of the first two rows correspond to hopper = No. (b) estimated intercepts and slopes for year x presence/absence of a hopper, based on the coefficient values shown in (a). All estimated coefficients ('Value') and their standard errors ('Std. Error') are on the scale of the Box-Cox transformation.

(a)

Fixed effects	Value	Std. Error	p-value
Intercept	-0.36124	0.096427	0.0002
p_RDL slope	0.751707	0.050331	< 0.0000
Hopper added intercept	0.23421	0.115164	0.0519
Year effect (2024)	-0.13583	0.041447	0.0015
Hopper added slope	0.211032	0.060374	0.0005
Random effect distribution s.d.	Lower CI	Estimate	Upper CI
Vessel	0.079157	0.133929	0.226601
Trip, within vessel	0.156690	0.189667	0.229583
Within-group	0.262893	0.277027	0.291922

(b)

	No hopper	Hopper
2023		
Intercept	-0.3612	-0.1270
p_RDL slope	0.7517	0.9627
2024		
Intercept	-0.497	-0.2628
p_RDL slope	0.7517	0.9627

TABLE 9. Fixed effect coefficients from the mixed-effects model fitted separately to each year. For 2023, there were 432 wells of 28 vessels and 66 trips. For 2024, there were 398 wells of 22 vessels and 61 trips. The p-values shown correspond to t-tests of the fitted coefficients. The intercept and slope coefficients shown in the first two rows for each year correspond to hopper = No. All estimated coefficients ('Value') and their standard errors ('Std. Error') are on the scale of the Box-Cox transformation.

2023	Value	Std. Error	p-value	Hooper present: intercept	Hopper present: p_RDL slope
intercept	-0.2635043	0.12126185	0.0304		
p_RDL slope	0.7750724	0.06775058	< 0.0000		
Hopper added intercept	0.0902458	0.14312845	0.5339		
Hopper added slope	0.1710522	0.08035681	0.0340		
				-0.1733	0.9461
2024					
intercept	-0.5585165	0.13258634	< 0.0000		
p_RDL slope	0.7603521	0.07460394	< 0.0000		
Hopper added intercept	0.4115028	0.16596485	0.0222		
Hopper added slope	0.2385667	0.09060553	0.0089		
				-0.1470	0.9989

a)



b)



FIGURE 1. (a) double-mesh brailer filled with fish; and, (b) a hopper on the main deck of a vessel.

FIGURA 1. (a) Salabardo de malla doble lleno de pescado; b) una tolva en la cubierta principal de un buque.

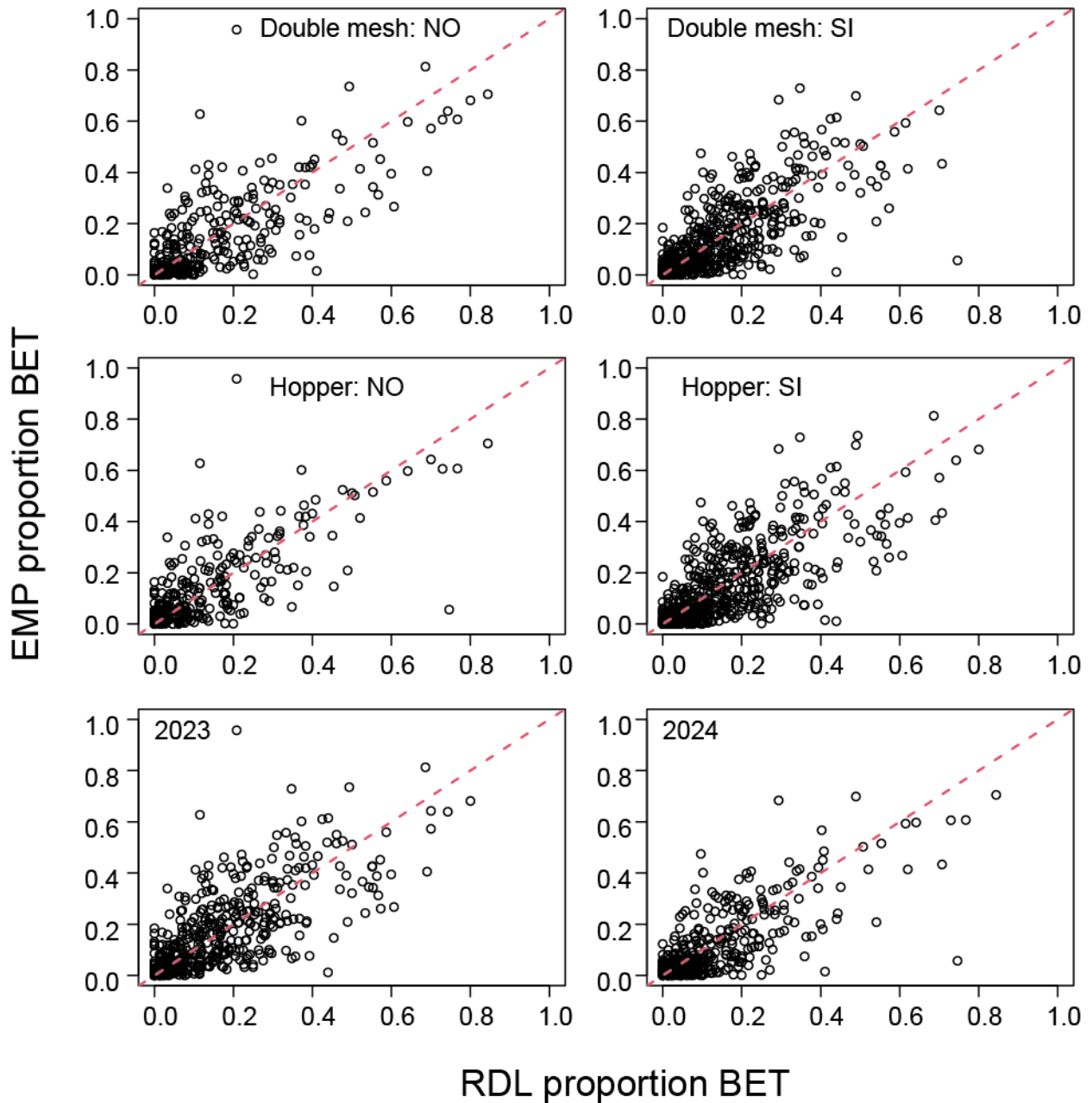


FIGURE 2. Paired estimates of the proportion of BET in each well, according to: presence/absence of double mesh on the brailer (top row); presence/absence of a hopper onboard the vessel (middle row); year the well was unloaded (bottom row). Each open circle is a well. The dashed red line is the 1-to-1 line.

FIGURA 2. Estimaciones pareadas de la proporción de BET en cada bodega, según: presencia/ausencia de malla doble en el salabardo (fila superior); presencia/ausencia de tolva a bordo del buque (fila central); año de descarga de la bodega (fila inferior). Cada círculo abierto corresponde a una bodega. La línea roja discontinua es la línea 1 a 1.

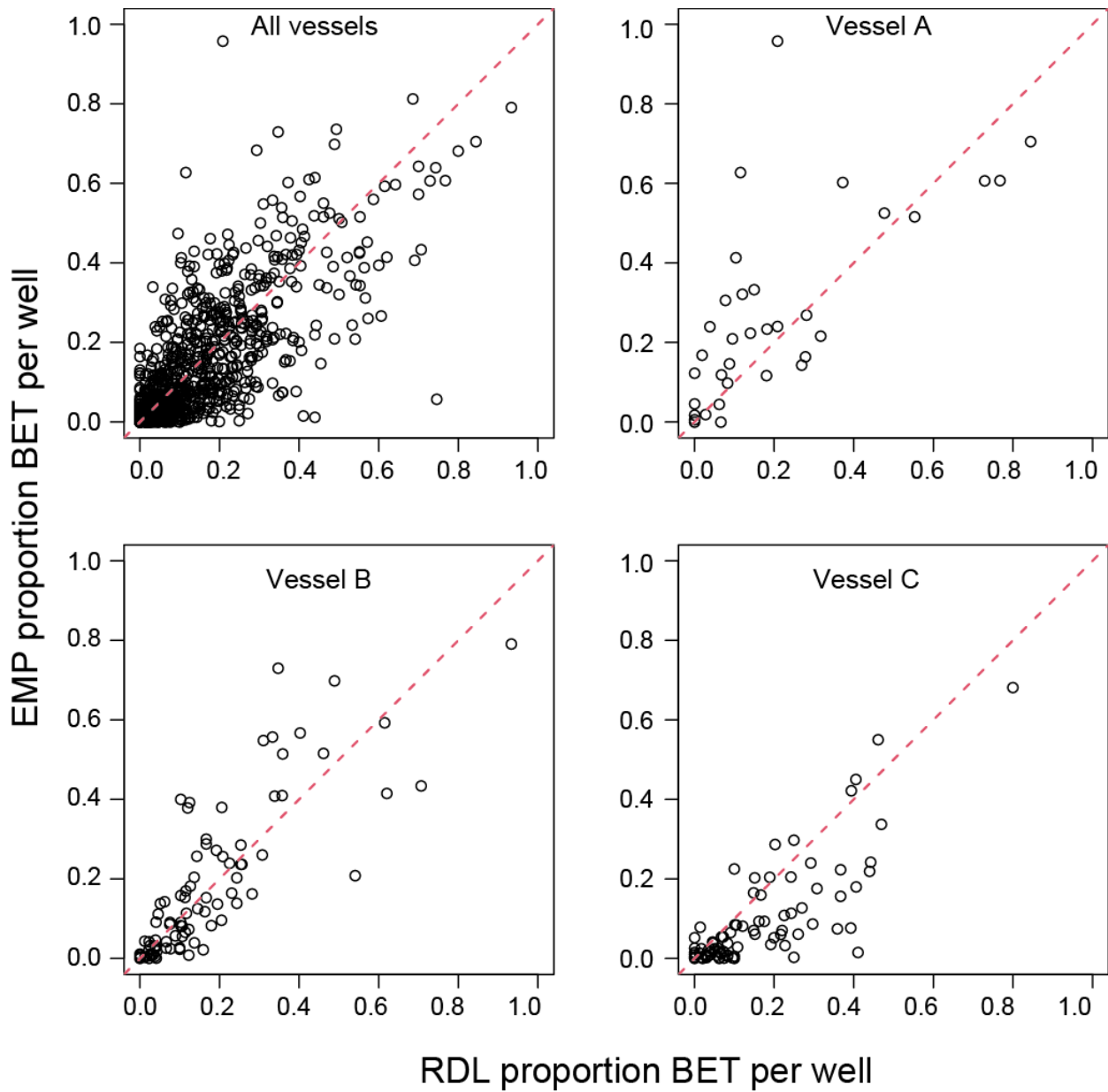


FIGURE 3. Plots of the paired estimates of the proportion of BET in the well, for all vessels, and for three example vessels, Vessels A, B, and C. Each open circle is a well. The red dashed line is the 1-to-1 line.

FIGURA 3. Gráficas de las estimaciones pareadas de la proporción de BET en la bodega, para todos los buques y para tres buques de ejemplo (los buques A, B y C). Cada círculo abierto es una bodega. La línea roja discontinua es la línea 1 a 1.

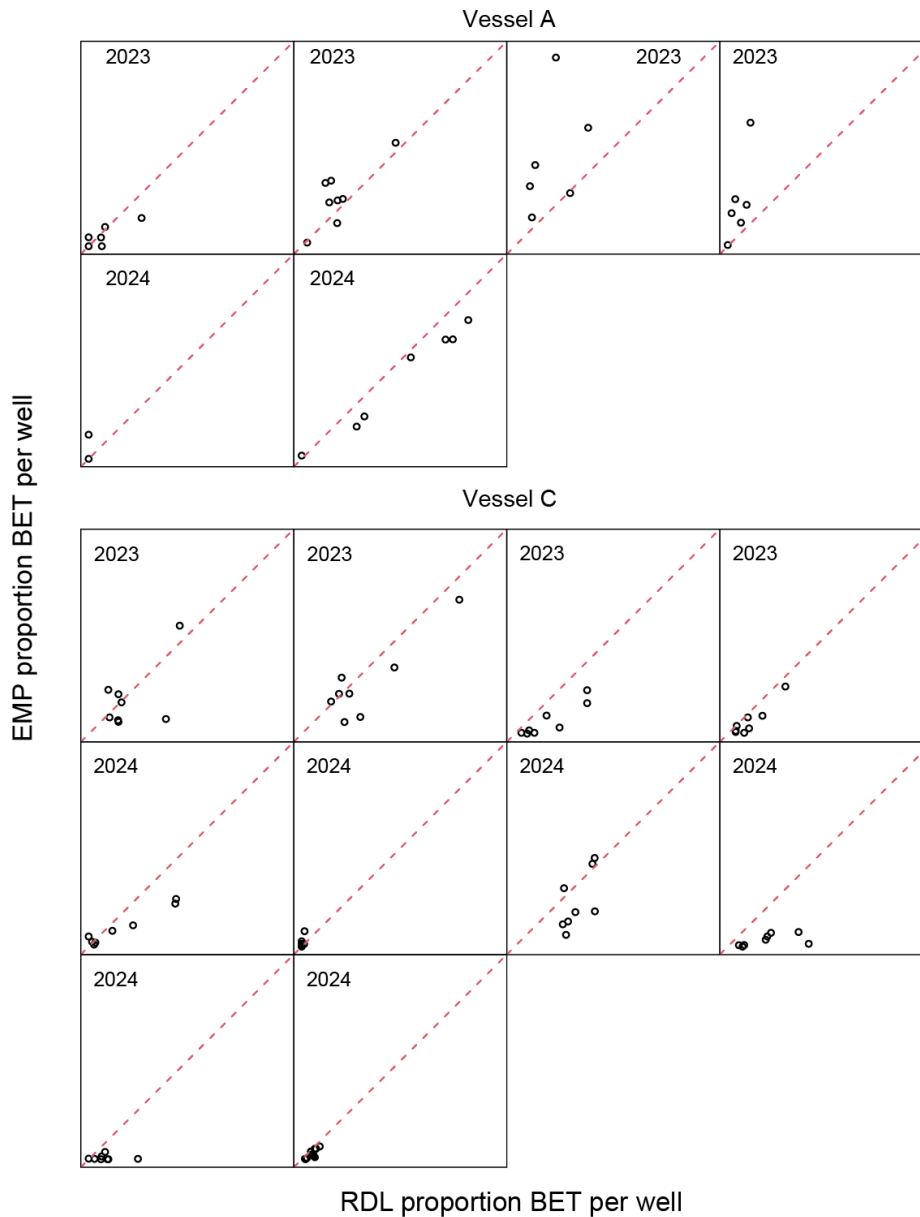


FIGURE 4. Trip-level plots of the paired estimates of the proportion of BET in the well, for two of the three example vessels shown in Figure 3. The range of both the x-axes and y-axes is the same for all panels, from 0 to 1. The red dashed lines are the 1-to-1 lines. Each open circle is an individual well, each panel shows the data for one trip. Panels are arranged by date of unloading; the year of unloading is shown in the lower right corner. The plots of data for all trips, for vessels A and C are shown in Figure 3.

FIGURA 4. Gráficas a nivel de viaje de las estimaciones pareadas de la proporción de BET en la bodega, para dos de los tres buques de ejemplo mostrados en la Figura 3. El rango de los ejes 'x' y 'y' es el mismo para todos los paneles, de 0 a 1. Las líneas rojas discontinuas son las líneas 1 a 1. Cada círculo abierto es una bodega individual, cada panel muestra los datos de un viaje. Los paneles están ordenados por fecha de descarga; el año de descarga aparece en la esquina inferior derecha. En la Figura 3 se muestran las gráficas de los datos de todos los viajes de los buques A y C.

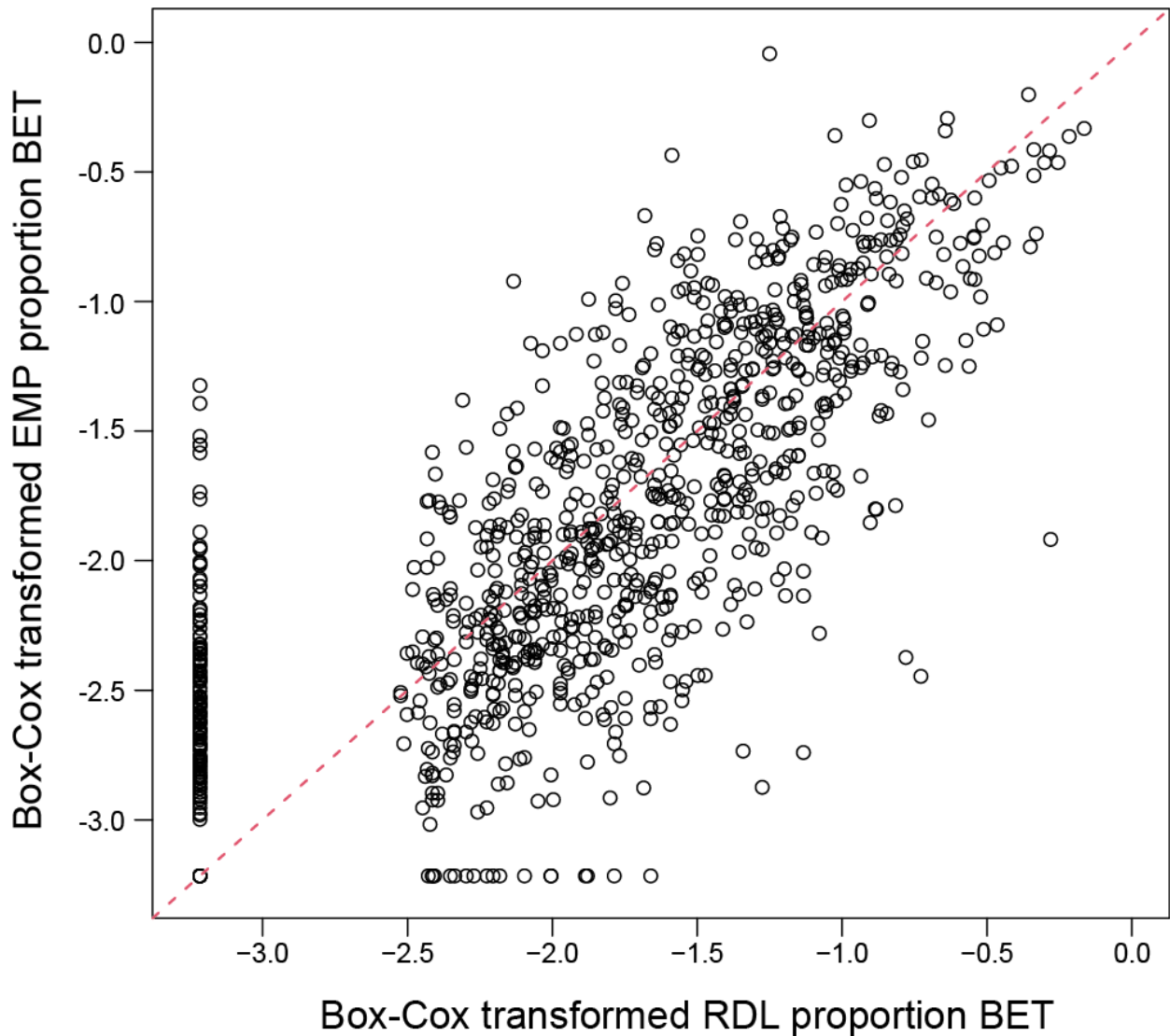


FIGURE 5. Paired Box-Cox transformed estimates of the proportion of BET in each well. A proportion of 0 corresponds to a Box-Cox-transformed value of about -2.7 and a proportion of 0.11 to a Box-Cox-transformed value of roughly -1.50. Each open circle is a well. The dashed red line is the 1-to-1 line.

FIGURA 5. Estimaciones pareadas transformadas mediante Box-Cox de la proporción de BET en cada bodega. Una proporción de 0 corresponde a un valor transformado mediante Box-Cox de aproximadamente -2.7 y una proporción de 0.11 a un valor transformado mediante Box-Cox de aproximadamente -1.50. Cada círculo abierto es una bodega. La línea roja discontinua es la línea 1 a 1.

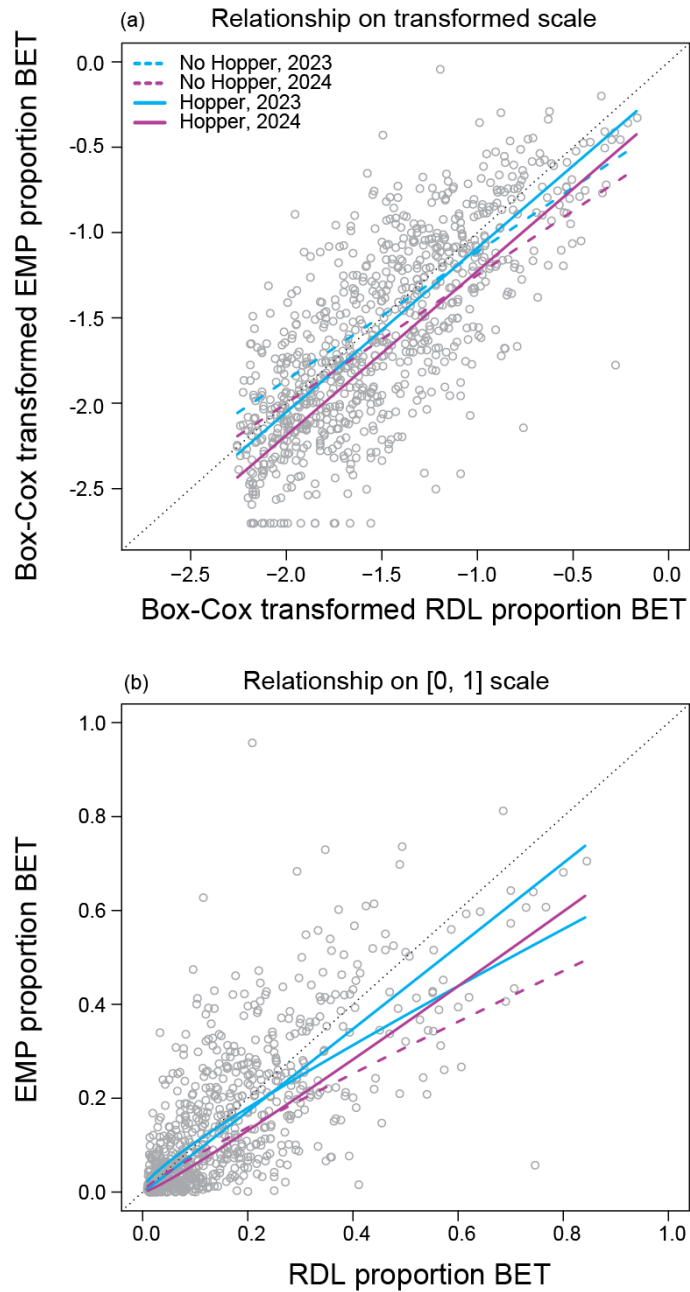


FIGURE 6. The fitted relationships from the mixed-effects model shown in Table 8a. (a): fitted lines on the scale of the Box-Cox transformation; (b): back-transformed relationships (i.e. on [0, 1] scale). The open gray circles are individual wells.

FIGURA 6. Las relaciones ajustadas del modelo de efectos mixtos mostrado en la Tabla 8a. (a): líneas ajustadas en la escala de la transformación Box-Cox; (b): relaciones retrotransformadas (es decir, en la escala [0, 1]). Los círculos grises abiertos son bodegas individuales.

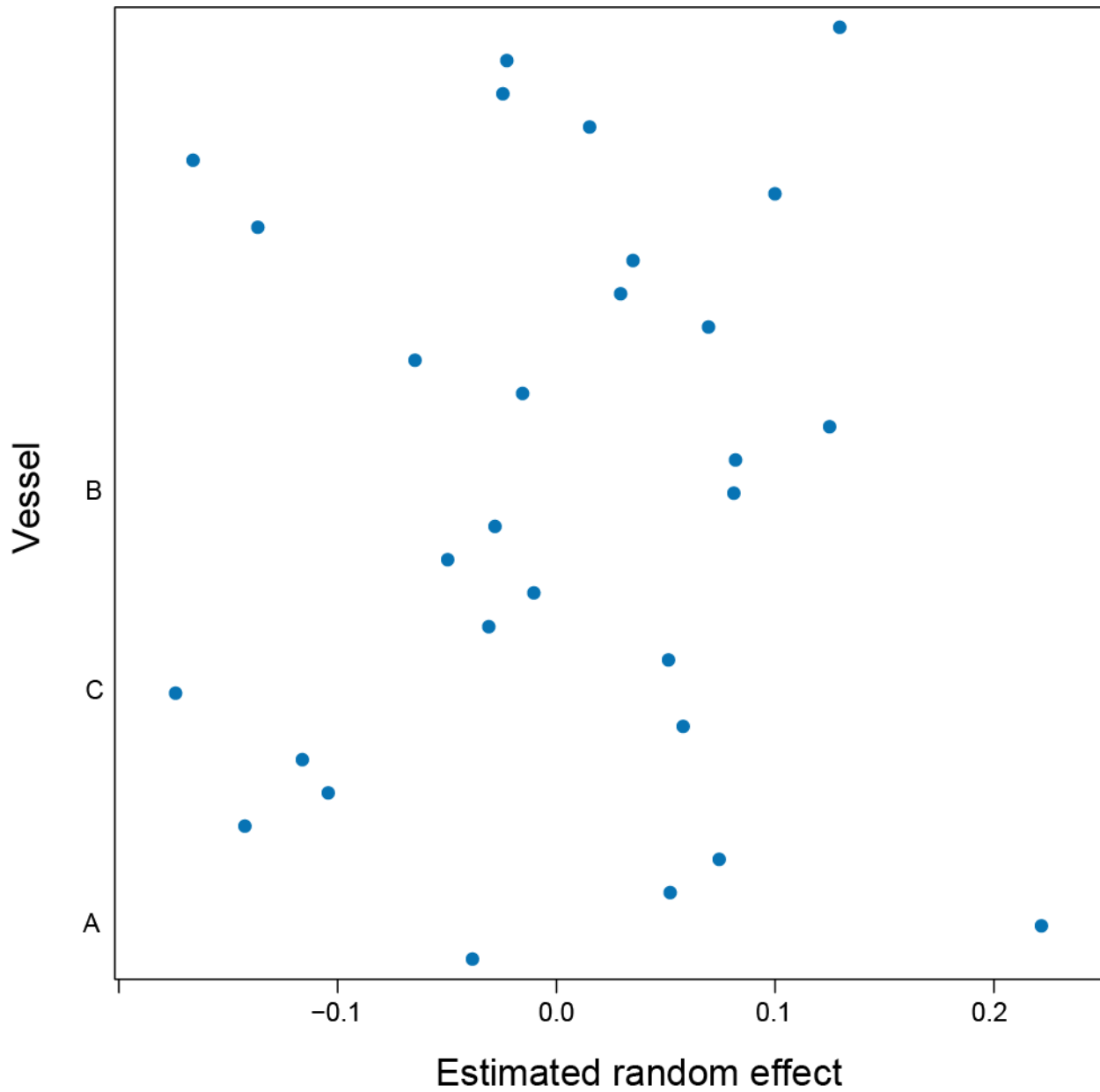


FIGURE 7. Estimated random effects (BLUPs) for each vessel for the mixed-effects model of Table 8a.

FIGURA 7. Efectos aleatorios estimados (MPLI) para cada buque para el modelo de efectos mixtos de la Tabla 8a.

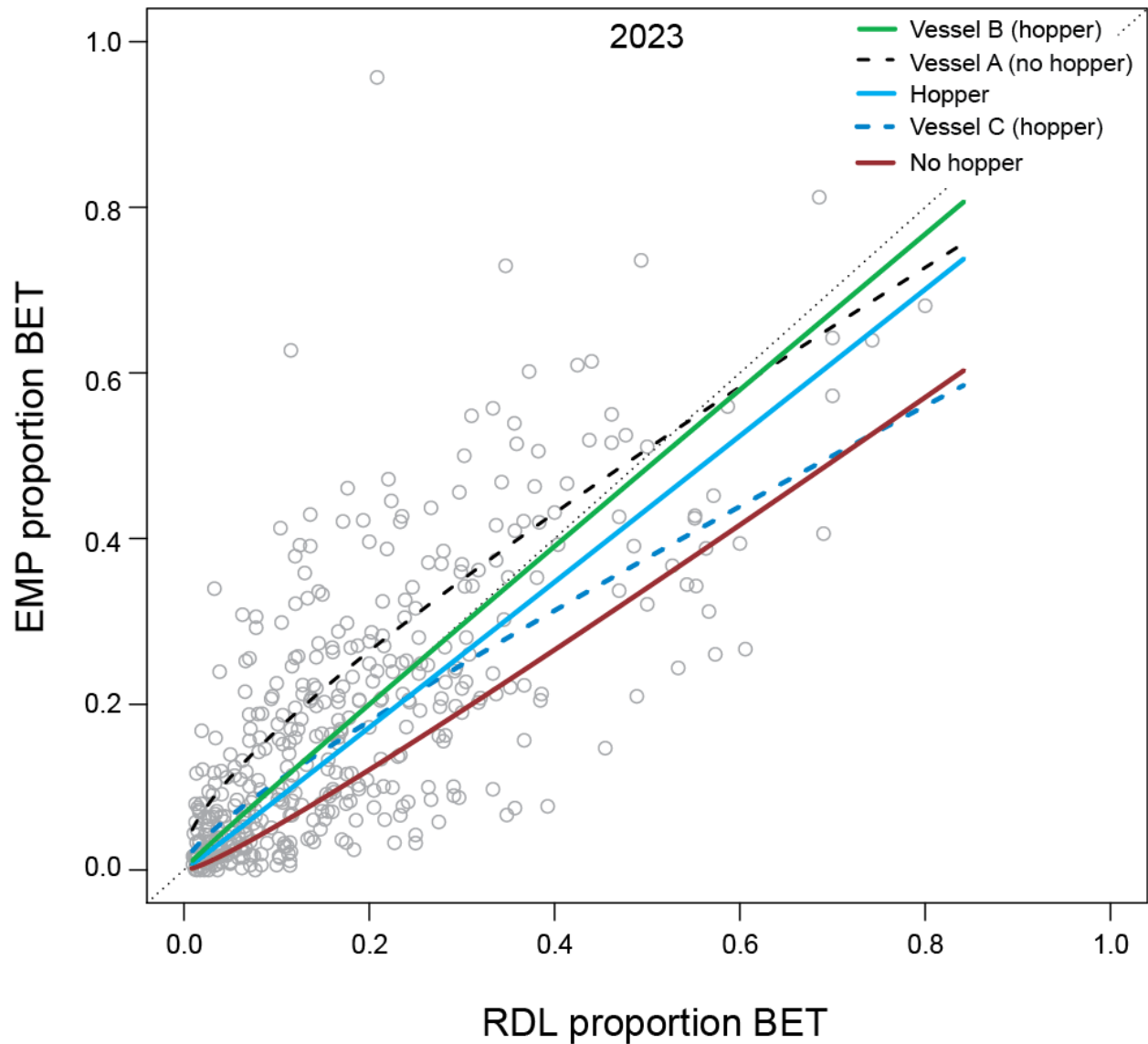


FIGURE 8. The fitted curves from the mixed-effects model shown in Table 8a for the three example vessels of Figures 3 – 4, for wells unloaded in 2023, on the [0, 1] scale. The population curves ('Hopper' and 'No Hopper') are from Figure 6b. The open gray circles are individual wells (trips unloading in 2023).

FIGURA 8. Las curvas ajustadas del modelo de efectos mixtos mostrado en la Tabla 8a para los tres buques de ejemplo de las Figuras 3-4, para bodegas descargadas en 2023, en la escala [0, 1]. Las curvas de población ('Tolva' y 'Sin tolva') proceden de la Figura 6b. Los círculos grises abiertos son bodegas individuales (viajes descargados en 2023).

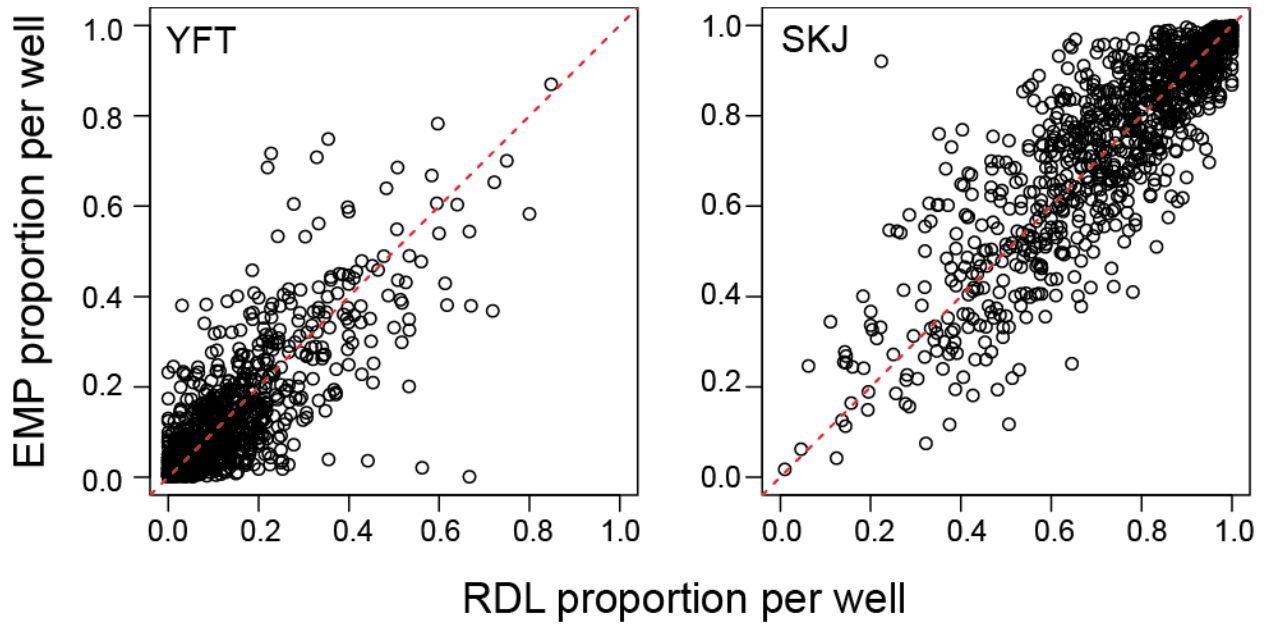


FIGURE 9. Paired estimates (EMP and RDL) of the proportion of YFT in each well (lefthand figure) and the proportion of SKJ in the well (righthand figure) for all vessels, 2023-2024. Each open circle is an individual well. The dashed red line is the 1-to-1 line.

FIGURA 9. Estimaciones pareadas (PRM y RDL) de la proporción de YFT en cada bodega (figura de la izquierda) y de la proporción de SJK en la bodega (figura de la derecha) para todos los buques, 2023-2024. Cada círculo abierto es una bodega individual. La línea roja discontinua es la línea 1 a 1.

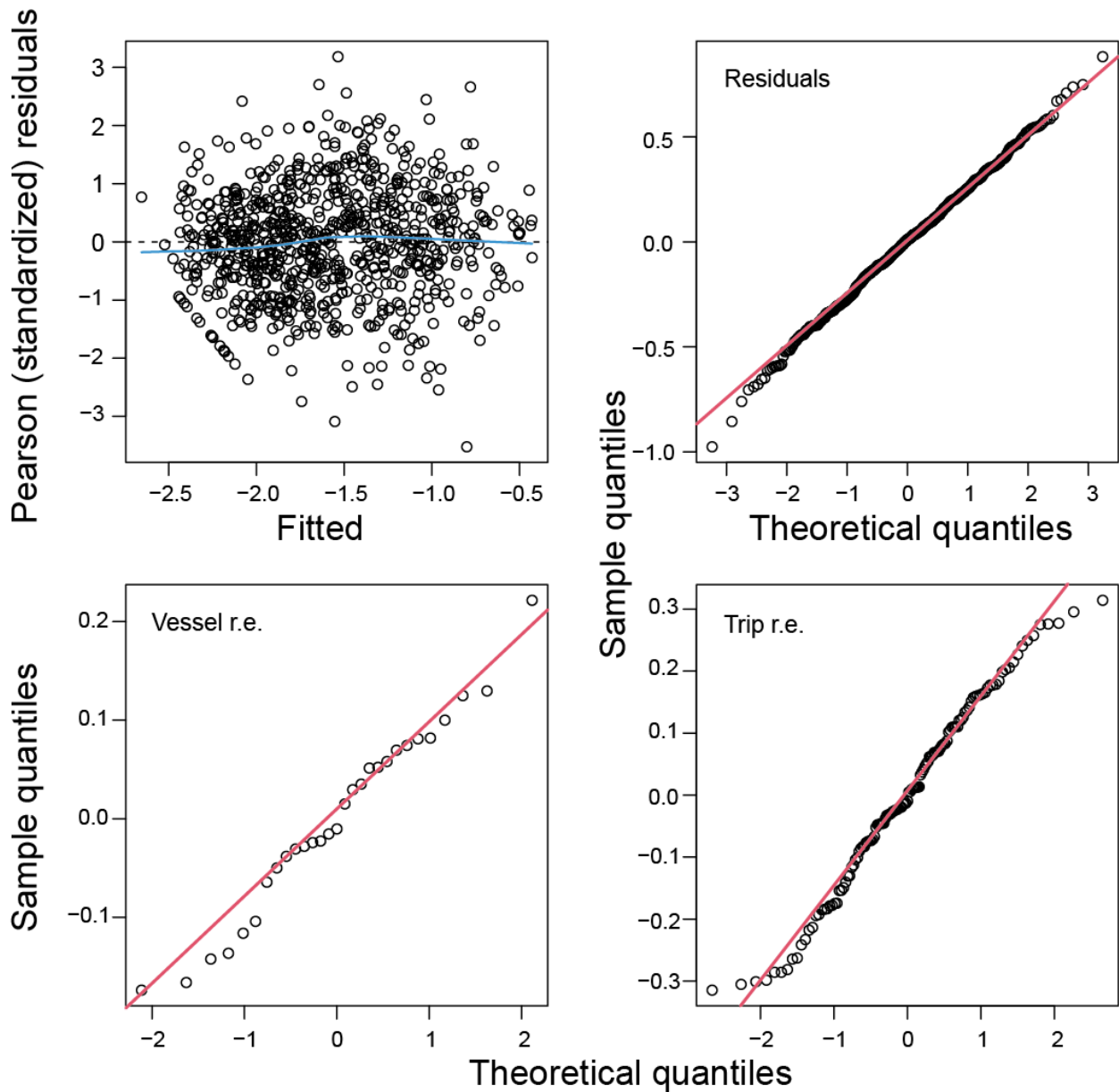


FIGURE 10. Diagnostic plots for mixed-effects model of Table 8a. “r.e.”: random effects. The blue line in the upper left panel is a loess smooth (span = 0.75, degree = 1). To aid with visualization of departures from normality, the red lines indicate a theoretical normal quantile-quantile relationship (passing through the first and third quartiles of the data).

FIGURA 10. Gráficas de diagnóstico para el modelo de efectos mixtos de la Tabla 8a. “r.e.”: efectos aleatorios. La línea azul en el panel superior izquierdo es un loess suavizado (span = 0.75, grado = 1). Para ayudar a visualizar las desviaciones de la normalidad, las líneas rojas indican una relación cuantil-cuantil normal teórica (que pasan por el primer y tercer cuartil de los datos).

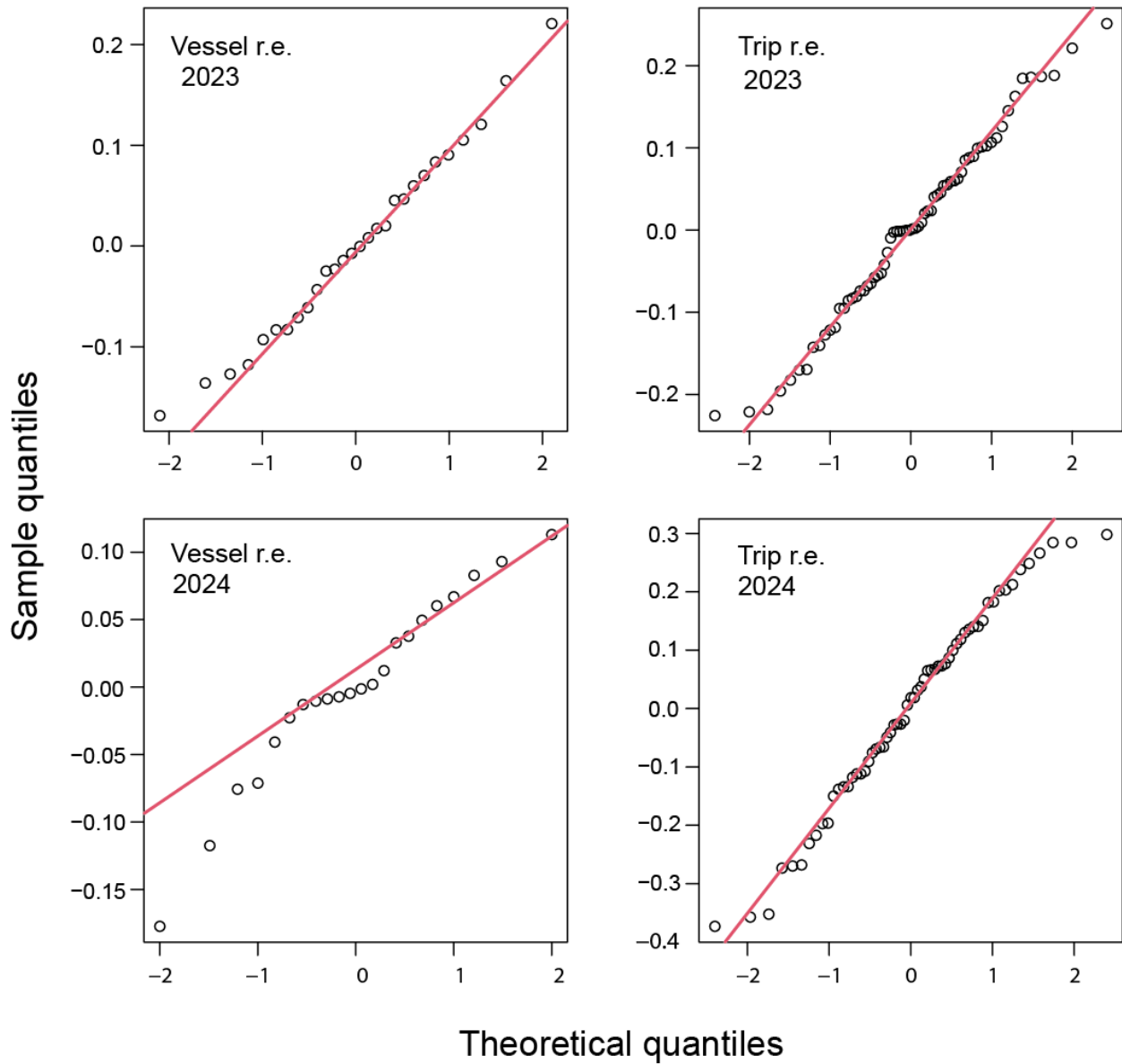


FIGURE 11. Quantile-quantile plots of the vessel random effects and trip random effect for the mixed-effects model of Table 8, fitted to 2023 and 2024 separately. To aid with visualization of departures from normality, the red lines indicate a theoretical normal quantile-quantile relationship (passing through the first and third quartiles of the data).

FIGURA 11. Gráficas de cuantil-cuantil de los efectos aleatorios de buque y de viaje para el modelo de efectos mixtos de la Tabla 8, ajustado a 2023 y 2024 por separado. Para ayudar a visualizar las desviaciones de la normalidad, las líneas rojas indican una relación cuantil-cuantil normal teórica (que pasan por el primer y tercer cuartil de los datos).